Equation of state of cubic boron nitride at high pressures and temperatures

F. Datchi,[1,*] A. Dewaele,[2] Y. Le Godec,[1] and P. Loubeyre[2]
[1]*IMPMC, Université Pierre et Marie Curie, CNRS, 140 rue de Lourmel, Paris F-75015, France*
[2]*DIF/DPTA, CEA, BP12, Bruyères-Le-Châtel F-91680, France*
(Received 27 February 2007; published 6 June 2007)

We report accurate measurements of the equation of state (EOS) of cubic boron nitride by x-ray diffraction up to 160 GPa at 295 K and 80 GPa in the range 500–900 K. Experiments were performed on single crystals embedded in a quasihydrostatic pressure medium (helium or neon). Comparison between the present EOS data at 295 K and literature allows us to critically review the recent calibrations of the ruby standard. The full *P-V-T* data set can be represented by a Mie-Grüneisen model, which enables us to extract all relevant thermodynamic parameters: bulk modulus and its first pressure derivative, thermal expansion coefficient, and thermal Grüneisen parameter and its volume dependence. This equation of state is used to determine the isothermal Grüneisen mode parameter of the Raman TO band. A formulation of the pressure scale based on this Raman mode, using physically constrained parameters, is deduced.

DOI: 10.1103/PhysRevB.75.214104 PACS number(s): 62.50.+p, 61.10.Nz, 65.40.De

I. INTRODUCTION

Cubic boron nitride (*c*-BN) is a material with remarkable properties: extreme hardness, chemical inertness, large band gap, and high mechanical and thermal stabilities. This makes it very attractive for a number of applications including abrasive or protective-coating material and microelectronic devices. Knowing the properties of *c*-BN under conditions of high pressure (P) and temperature (T) is important for some of these applications. It has also been recognized[1,2] that *c*-BN could be a useful pressure sensor in high-pressure (HP)–high-temperature (HT) experiments in diamond-anvil cells, based on its intense Raman TO band (1054 cm^{-1} at ambient conditions) which is well separated from the signal of the anvils. This has recently motivated investigations of the Raman spectra under extreme conditions of P and T.[3–5]

As pointed out by Holzapfel,[6] the accurate determination of the equation of state (EOS) of solids with very large bulk modulus is a stringent test for the ruby sensor calibration, a matter which has been under intensive debate recently.[6–12] For highly incompressible solids such as *c*-BN, experiments in the megabar range are required in order to extract reliable values of the bulk modulus B_0 and its first pressure derivative B_0'. At ambient temperature, the equation of state has been so far investigated up to 34 GPa in a He pressure medium,[1] to 66 GPa in N_2,[13] and 120 GPa in methanol-ethanol.[14] Although the maximum pressure in the latter study is relatively high, the small number of measurements, their limited accuracy, and the use of a pressure media prone to nonhydrostatic stress above ~20 GPa (Ref. 15) reflect in poorly constrained and questionable values of B_0 and B_0'.

There is to date no available EOS data at simultaneous high pressure and temperature. By contrast, several theoretical studies[16–18] have reported thermal properties at ambient and high pressures. These works relied on the assumption that *c*-BN can be treated as a quasiharmonic solid; this still needs to be validated by experiment.

We present here careful and accurate measurements of the EOS up to 160 GPa at 295 K and up to 80 GPa at high temperatures (500–900 K). We used helium or neon (at high T) as pressure transmitting medium, since they are known to provide the closest approximation to hydrostatic compression in the megabar range.[9,15] The thermal expansion at ambient pressure has also been investigated to 950 K. We show that our data can be represented by a simple Mie-Grüneisen model. This allows us to extract all the relevant thermodynamic parameters. The EOS is then used to determine the isothermal Grüneisen parameter of the Raman TO band. Accordingly, the pressure scale based on this Raman band is reformulated using physical constraints.

This paper is organized as follows. In Sec. II, we present the experimental procedure. Section III is devoted to the presentation of the room-temperature equation of state. The thermal expansion at room pressure follows in Sec. IV. The presentation and analysis of *P-V-T* data at simultaneous HP-HT are given in Sec. V. In Sec. VI, the thermal dependence of the isothermal Grüneisen parameter of the Raman TO band is investigated and a formulation of the Raman pressure scale is then presented. Section VII finally gives concluding remarks.

II. EXPERIMENTAL PROCEDURE

The present experiments were conducted with single crystals of *c*-BN of size ranging from 3 to 15 μm. These were selected from a powder batch using their Raman signal as a criterion for good crystallinity: crystals which presented intense Raman first-order TO and LO bands with Lorentzian shapes and small bandwidths (~5 cm^{-1}) were selected. A few crystals were then loaded into the experimental volume of a diamond-anvil cell, along with ruby and $SrB_4O_7:Sm^{2+}$ as pressure sensors. Care was taken in order to position the samples and the pressure sensors within a few micron distance to each other and at the center of the diamond culet. We used diamond anvils with flat culets of 0.1–0.4 mm and rhenium gaskets. Helium was chosen as pressure transmitting medium for the room-temperature experiments above 50 GPa and neon was used otherwise. In the *P-T* range of the present experiments, these two pressure transmitting me-

dia are known to provide the best approximation to hydrostatic conditions.[9,15]

Membrane diamond-anvil cells (MDACs) designed for high-temperature operation were used. The cells could be fitted as a whole inside a ring-shaped resistive heater. To achieve temperatures above 800 K, a smaller, additional heater made of a resistive wire coiled around a ceramic tube is positioned around the anvil-gasket assembly. The temperature of the heaters is regulated within 1 K using commercial devices. An isolated, *K*-type thermocouple is fixed by ceramic cement with its head in contact with the diamond anvil, close to the gasket. The ensemble is heated in air or in an Ar-H_2(2%) reducing atmosphere. Numerous previous experiments have shown that the temperature measured by the thermocouple is within 5 K of the sample temperature.[3,19,20]

Pressure was determined using the pressure shift of the luminescence lines of ruby (at 295 K) or $SrB_4O_7:Sm^{2+}$. The pressures reported here are based on Holzapfel's 2005 ruby scale,[11] hereafter denoted as H2005. We also compared the results obtained with other ruby calibrations,[6,10–12,21] and, as discussed below, H2005 was found to provide excellent consistency between present and literature data. The calibration of the $SrB_4O_7:Sm^{2+}$ sensor,[22] initially based on the ruby scale from Ref. 21, was also modified to match the H2005 scale. For the measurements above 100 GPa at 295 K, the ruby signal was too weak; thus, the pressure was determined from the equation of state of ^{4}He (Ref. 23, with proper correction for the H2005 ruby scale). The volume of ^{4}He was calculated using the reflections present on the same diffraction patterns as the *c*-BN sample, and excellent agreement between this pressure determination and that from ruby was observed below 100 GPa.

Angular-dispersive x-ray-diffraction experiments were performed on beamline ID27 of the European Synchrotron Radiation Facility (ESRF, Grenoble, France). The monochromatic beam (λ=0.3738 Å) was focused to an $\approx 7\times 10$ μm^2 spot. Diffracted x rays were collected by a MAR345 image plate, while the MDAC was continuously rotated about the ϕ axis by ±20°. The images were integrated using the FIT2D program.[24] Between six and nine single-crystal reflections could be observed depending on the sample, with a resolution of up to ≈0.83 Å. All of them could be indexed in the zinc-blende structure (space group $F\bar{4}3m$) reported for this material.[25] The lattice parameter *a* was refined with the program UNITCELL (Ref. 26) using the measured *d* spacings of all observed reflections. The uncertainty on *a* was on average 5×10^{-4} Å.

III. ROOM-TEMPERATURE EQUATION OF STATE

The volume per atom *V* of *c*-BN at 295 K ($V=a^3/8$) was measured up to 57.8 GPa in a neon pressure medium and up to 162 GPa in a helium pressure medium. Excellent agreement is observed between the two data sets. The results are gathered in Fig. 1 and Table IV. As expected, no phase transition was observed in this pressure range.

To extract the values of the zero-pressure isothermal bulk modulus B_0 and its first pressure derivative B_0' from the present data, we considered three different phenomenological models of equation of state: the Vinet form,[27] the Birch-Murnaghan second-order form,[28] and Holzapfel's AP2 equation.[29] These relations were least-squares fitted to the data. The results are listed in Table I, and the fit using the Vinet equation[27] is plotted in Fig. 1. In the compression range probed here ($0.77 \leqslant V/V_0 \leqslant 1$), the three models fit the data equally well and give very similar values for B_0 [395(2)–397(2) GPa] and its first pressure derivative B_0' [3.50(5)–3.62(5)]. Here, as in all the text, the number in parentheses indicate the standard deviation for the last digit of the fitting parameter; it does not reflect its absolute uncertainty, which primarily depends here on the absolute accuracy of the ruby standard. The volume and pressure difference between experimental data and the Vinet fit is shown in Fig. 2. The volume V_0 at $P=0$ and 295 K was taken as the measured value at 1 atm of 5.9062(6) Å^3/at., corresponding to a lattice parameter a_0 of 3.6152(2) Å. The latter values are identical, within uncertainties, to previous reports.[1,14,30]

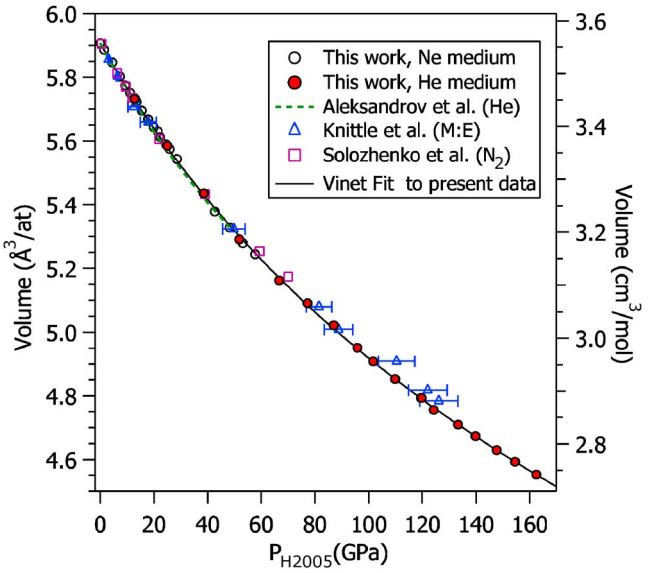

FIG. 1. (Color online) Volume per atom of *c*-BN as a function of pressure at 295 K. The open and solid circles are present measurements on samples in neon and helium pressure media, respectively. The estimated error bars are within the symbol sizes. Triangles, Ref. 14 (in methanol and/or ethanol); dashed line, Ref. 1 (in helium); squares: Ref. 13 (in nitrogen). The solid line is the fit to the present data using the Vinet equation (Ref. 27) [V_0=5.9062(6) Å^3/at., B_0=395(2) GPa, and B_0'=3.62(5)].

Figures 1 and 2 also show experimental data obtained in previous studies.[1,14] For comparison with the present work,

TABLE I. Comparison between values for the zero-pressure isothermal bulk modulus B_0 and its first pressure derivative B_0' obtained by fitting the present data at ambient temperature to different EOS models: Vinet (Ref. 27), second-order Birch-Murnaghan (BM) (Ref. 28), and Holzapfel's AP2 form (Ref. 29). The zero-pressure volume V_0(295 K) was fixed to 5.9062 Å^3/at.

Model	Vinet	BM	AP2
B_0 (GPa)	395(2)	396(2)	397(2)
B_0'	3.62(5)	3.54(5)	3.50(5)

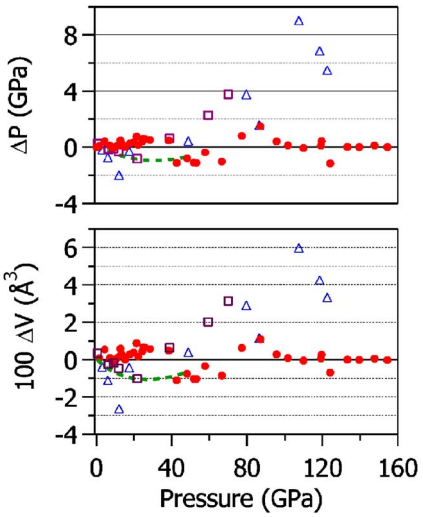

FIG. 2. (Color online) Comparison between experimental data at 295 K from this work (circles), Ref. 14 (triangles), Ref. 13 (squares), and Ref. 1 (dashed line). The fit to the present data using the Vinet EOS (Ref. 17) is used as the reference. The top graph shows the difference in pressure and the bottom one, the difference in volume multiplied by a factor of 100.

the original pressure values have been rescaled onto the H2005 scale. Aleksandrov *et al.*[1] reported their measurements up to 34 GPa in He in the form of a quadratic fit of the compression factor $\Delta\rho/\rho_0$, where ρ is the density, vs the relative shift of the ruby R_1 line. Their absolute volume values differ from ours by less than 2×10^{-2} Å^3/at., corresponding to a maximum pressure difference of 2 GPa. By contrast, systematic deviations are observed between our measurements and those of Solozhenko *et al.*[13] and Knittle *et al.*[14] above about 40 GPa, where their measured volume at a given pressure is systematically higher than ours. This is likely due, at least in part, to the larger nonhydrostatic stresses produced by the N_2 or methanol-ethanol pressure medium used in the experiments of Solozhenko *et al.*[13] and Knittle *et al.*,[14] respectively.

As mentioned above, the values of B_0 and B_0' obtained by fitting the EOS of highly incompressible solids such as *c*-BN and diamond are very sensitive to the chosen pressure calibration for the ruby standard. As a matter of fact, the first hint that the commonly used 1986 calibration of Mao *et al.*[21] (hereafter denoted as MXB1986) becomes increasingly wrong with pressure was given by the measurements of the diamond EOS by Aleksandrov *et al.*[1] to 40 GPa in 1989. More recently, the very accurate measurements of the diamond EOS up to megabar pressures by Occelli *et al.*[7] evidenced more firmly the discrepancy between the value found for B_0' using ultrasonic techniques (4.0±0.7), on one hand, and that obtained from the EOS (3.0) when pressure is calculated with the MXB1986 scale, on the other hand. Consequently, a revision of the latter scale has been proposed by several authors[6,8–12] based on the diamond data and/or those recently obtained for the EOS of several metals that showed the same trend.[9]

In Table II, we compare the B_0 and B_0' parameters obtained by fitting the Vinet EOS to the present *c*-BN data using the various ruby calibrations proposed in the literature. For comparison and consistency check, we also show the results obtained with the diamond data of Occelli *et al.*[7] To decide which ruby scale(s) seems (seem) more reasonable, we list in Table III the values of B_0 and B_0' determined by other means, whether experimental (ultrasonic or Brillouin scattering measurements) or theoretical. Unfortunately, there exists only one determination of B_0' for diamond using ultrasonic experiments under pressure, which has a limited accuracy, and none has been reported yet for *c*-BN. The largest source of comparison thus comes from the numerous theoretical studies based on first-principles (*ab initio*) techniques. Whereas the bulk modulus and zero-pressure volume show large variations among the various theoretical studies, the values for B_0' appear much less dependent on the theoretical approaches and approximations used in each of them, espe-

TABLE II. Comparison between values of B_0 (in GPa) and B_0' of *c*-BN and natural diamond (C) at 295 K obtained with different ruby scales from the literature. B_0 and B_0' are determined by fitting the present data (*c*-BN) and data of Occelli *et al.* (C) to the Vinet model (Ref. 27). In all fits, the values of the zero-pressure volume were fixed to 5.9062 Å^3/at. (*c*-BN) and 5.6733 Å^3/at. (C). χ^2 indicates the goodness of fit.

	c-BN			Diamond		
Ruby scale	B_0	B_0'	χ^2	B_0	B_0'	χ^2
MXB1986[a]	397(3)	2.75(6)	14.2	447(3)	3.00(7)	4.5
AGSY1989[b]	394(3)	3.93(7)	21	440(3)	4.38(8)	6.4
H2003[c]	390(2)	3.49(5)	12.1	435(2)	3.87(4)	1.5
DLM2004[d]	395(3)	3.28(6)	16.8	440(3)	3.66(7)	4.6
H2005[e]	395(2)	3.62(2)	12.8	443(3)	3.97(5)	1.5
CNSS2005[f]	387(3)	3.64(7)	18.2	432(3)	4.05(7)	5.3
DO2007[g]	398(2)	3.35(5)	13.6	444(2)	3.72(5)	2.6

[a]Reference 21.
[b]Reference 1.
[c]Reference 6.
[d]Reference 9.
[e]Reference 11.
[f]Reference 10.
[g]Reference 12.

TABLE III. Literature data for the values of V_0, B_0, and B_0' of *c*-BN and diamond (^{12}C). V_0 is in Å^3/at. and B_0 in GPa. The various abbreviations are DFT (density-functional theory), LDA (local-density approximation), GGA (generalized gradient approximation), ZPE (zero-point energy), DG (Debye-Grüneisen model), LD (lattice dynamics), VMC (variational quantum Monte Carlo), DMC (diffusion quantum Monte Carlo), and QHA (quasiharmonic approximation); "static" stands for calculations of the static lattice.

c-BN					^{12}C				
Reference	V_0	B_0	B_0'	Method	Reference	V_0	B_0	B_0'	Method
31		400(20)		Brillouin	32		442(5)	4.0(7)	Ultrasound
16	5.797	395	3.65	DFT+LDA (static)	33		444.8(8)		Brillouin
	5.884	387	3.66	DFT+LDA+ZPE (0 K)	34	5.497	473	3.5	DFT+LDA (static)
	5.888	385	3.66	DFT+LDA+ZPE+DG (300 K)	8	5.510	465	3.63(3)	DFT+LDA (static)
18	5.745	391		DFT+LDA+LD (300 K)		5.697	433(2)	3.67(3)	DFT+GGA (static)
35	5.788	397	3.6	DFT+LDA (static)	36	5.529	454	3.65	DFT+LDA+ZPE+QHA (300 K)
17	5.742	398		DFT+LDA (static)		5.722	422	3.72	DFT+GGA+ZPE+QHA (300 K)
37	5.718	397	3.59	DFT+LDA (static)		5.604	472(4)	3.8(1)	VMC+ZPE+QHA (300 K)
14	5.954	368	3.6	DFT+LDA (static)		5.711	437(3)	3.7(1)	DMC+ZPE+QHA (300 K)
38	5.905	370	3.8	Tight binding					

cially if we consider the most recent works. Indeed, the two latest studies of diamond give values of B_0' between 3.65 and 3.8(1), whether the density-functional theory (DFT), within local-density approximation (LDA) or generalized gradient approximation (GGA), or the quantum Monte Carlo approach is used. Similarly, all DFT-LDA calculations on *c*-BN give $B_0'=3.6\pm0.05$, irrespective of the considered pseudopotential. In the case of *c*-BN also, there is a nice agreement between the latest studies on the values of B_0 which vary from 395 to 398 GPa, i.e., in very good agreement with the Brillouin scattering experiment[31] (400±20 GPa). We see from Table II that the ruby scales H2003, H2005, and DO2007 are those giving the best consistency with available literature data while providing the best fits based on the least-squares χ^2 criterion. The DLM2004 and CNSS2005 calibrations give close results but a larger χ^2, which could be ascribed to the functional form used. This also confirms that the MXB1986 scale becomes increasingly wrong with pressure, underestimating it by about 8.8% at 160 GPa. We note that H2003, H2005, DLM2004, CNSS2005, and DO2007 scales agree within 3% at 160 GPa, which may be considered as the present uncertainty of the ruby scale at this pressure. It is now clear that independent experimental determination of B_0', such as given by sound-propagating experiments, for both *c*-BN and diamond could help to better establish the ruby scale in the megabar range.

IV. THERMAL EXPANSION AT AMBIENT PRESSURE

We performed volume measurements at room pressure as a function of temperature between 295 and 948 K. The results are plotted in Fig. 3 and reproduced in Table IV. They are compared to those of Slack and Bertram[30] between 77 and 1289 K. The two data sets agree within error bars in the overlapping range, although we systematically find larger volume values at a given temperature above 300 K. The calculations of Albe[16] are also shown as the dotted line in Fig. 3. They are based on the DFT within the LDA for the static part and a Debye-Grüneisen model for the thermal part. The calculated volume follows very well the experimental data below 500 K but increasingly overestimates them above this temperature.

The present data and data of Slack and Bertram[30] were fitted together using the second-order approximation to the zero-pressure Grüneisen equation of state (see Ref. 39 and references therein). In this approximation, the temperature dependence of the volume is given by

$$V_0(T) = V_{0,0}\left[1 + \frac{U_{th}(T)}{Q - bU_{th}(T)}\right], \tag{1}$$

where $U_{th}(T)$ is the internal energy due to lattice vibrations, $b=\frac{1}{2}(B_{0,0}'-1)$, and $Q=(V_{0,0}B_{0,0})/\hat{\gamma}$. $V_{0,0}$, $B_{0,0}$, and $B_{0,0}'$ are,

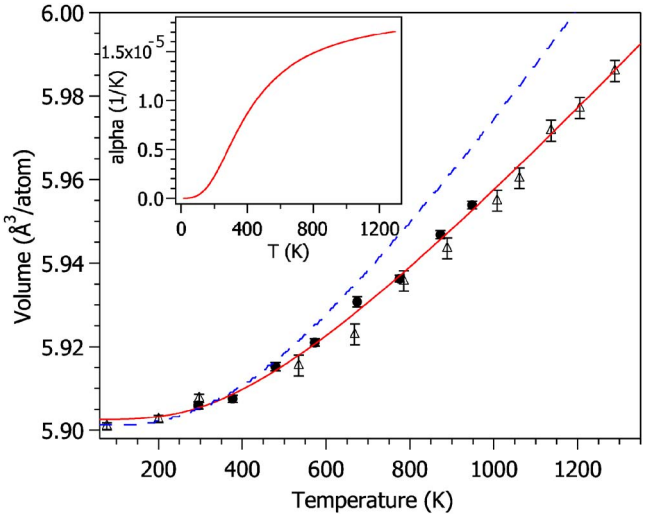

FIG. 3. (Color online) Volume and thermal expansion coefficient as a function of temperature. The solid circles are present data, and triangles show measurements of Ref. 30. The fit to both data sets using Eq. (1) is shown as the solid line. The dashed line represents the calculations of Albe (Ref. 16). In the inset, the volume thermal coefficient α_0 is represented.

TABLE IV. Experimental *P-V-T* data of *c*-BN obtained in the present work. *P* is in GPa, *a* in Å, *V* in Å^3/at., and *T* in K.

P	*T*	*a*	*V*	*P*	*T*	*a*	*V*
0.0	295	3.6152	5.907	0.0	377	3.6158	5.909
1.5	295	3.6110	5.886	0.0	479	3.6174	5.917
4.5	295	3.6029	5.846	9.8	497	3.5879	5.773
7.4	295	3.5938	5.802	21.6	499	3.5555	5.618
9.3	295	3.5880	5.774	2.0	500	3.6110	5.886
11.1	295	3.5832	5.751	25.1	500	3.5465	5.576
12.7	295	3.5792	5.732	13.9	500	3.5760	5.716
13.0	295	3.5793	5.732	46.5	501	3.4983	5.352
13.5	295	3.5771	5.721	44.5	501	3.5024	5.370
15.4	295	3.5715	5.695	0.0	573	3.6181	5.920
17.8	295	3.5658	5.667	39.3	600	3.5145	5.426
19.9	295	3.5607	5.643	47.9	600	3.4965	5.343
21.4	295	3.5578	5.629	56.5	600	3.4791	5.264
22.3	295	3.5541	5.612	66.3	600	3.4609	5.182
24.4	295	3.5494	5.590	76.2	600	3.4458	5.114
25.0	295	3.5484	5.585	84.2	600	3.4264	5.028
26.0	295	3.5461	5.574	0.0	674	3.6201	5.930
28.6	295	3.5395	5.543	8.2	748	3.5962	5.814
38.6	295	3.5164	5.435	4.6	748	3.6069	5.866
42.7	295	3.5040	5.378	18.9	749	3.5653	5.665
48.2	295	3.4930	5.327	35.8	749	3.5243	5.472
51.9	295	3.4849	5.290	42.1	750	3.5095	5.403
53.1	295	3.4823	5.278	49.5	750	3.4938	5.331
57.8	295	3.4746	5.244	14.7	750	3.5789	5.730
66.6	295	3.4565	5.162	0.0	775	3.6216	5.938
77.3	295	3.4405	5.091	0.0	873	3.6233	5.946
87.0	295	3.4249	5.022	54.2	900	3.4841	5.287
95.7	295	3.4087	4.951	0.0	948	3.6246	5.952
101.6	295	3.3989	4.908				
109.8	295	3.3860	4.853				
119.3	295	3.3722	4.793				
119.7	295	3.3721	4.793				
124.3	295	3.3634	4.756				
133.3	295	3.3525	4.710				
139.7	295	3.3437	4.673				
147.7	295	3.3334	4.630				
154.5	295	3.3246	4.593				
162.5	295	3.3147	4.553				

respectively, the volume, bulk modulus, and its first derivative at zero pressure and temperature. $\hat{\gamma}$ is the thermobaric Grüneisen parameter defined by

$$\hat{\gamma} = -(V/U_{th})(\partial F_{th}/\partial V)_T = (V/U_{th})P_{th}, \tag{2}$$

where $F_{th}(V,T)$ is the thermal part of the Helmholtz free energy and $P_{th}=-(\partial F_{th}/\partial V)_T$. If $\hat{\gamma}$ is independent of T, which we assume here, then $\hat{\gamma}=\gamma_{th}$ where γ_{th} is the thermodynamic Grüneisen parameter [$\gamma_{th}=(V/C_v)(\partial P/\partial T)_V$, with C_v the specific heat at constant volume].[39] $U_{th}(T)$ was evaluated within the Debye model as follows:

$$U_{th}(T) = 9RT\left(\frac{\Theta_0}{T}\right)^3 \int_0^{\Theta_0/T} \frac{x^3}{\exp(x)-1} dx, \tag{3}$$

where R is the ideal gas constant and Θ_0 the Debye temperature at $P=0$. For the latter, we used the value of 1700 K estimated from the infrared spectrum by Gielisse *et al.*,[40] which is also in agreement with the data on specific heat.[18,41]

$B_{0,0}$ was fixed at 397 GPa, which is obtained by adding to the value of B_0(295 K) found above (Vinet fit) the small correction (2 GPa) calculated by Albe[16] between 0 and 300 K (Table III). $B'_{0,0}$ was fixed equal to $B'_0(295\ \mathrm{K})=3.62$, as no variation was observed for this parameter in Albe's calculations[16] between 0 and 300 K.

The fit of the $V_0(T)$ data with Eq. (1) then gives $V_{0,0}=5.9026(4)$ Å^3/at. and $\gamma_{th,0}=1.04(1)$ [$\gamma_{th,0}=\gamma_{th}(P=0)$]. It is shown as the solid line in Fig. 3. The temperature dependence of the thermal expansion coefficient α_0, calculated by differentiating Eq. (1), is plotted in the inset of the same figure. It is seen that Eq. (1) gives a good reproduction of $V_0(T)$ in the considered temperature range. We note that the present value for $\gamma_{th,0}$ is close to the one obtained by Brillouin-zone integration of the phonon dispersion curve ($\langle\gamma_\nu\rangle=0.95$) determined by Kern *et al.*[17] using density-functional theory. The difference between experiment and Albe's calculations[16] of $V_0(T)$ mentioned above is also readily explained by the value of 1.3 used by this author for $\gamma_{th,0}$.

V. HIGH-PRESSURE AND -TEMPERATURE EQUATION OF STATE

High-pressure and -temperature measurements were performed up to 80 GPa at 500, 600, 750, and 900 K, with the results listed in Table IV. The *P-V-T* data set is represented in Fig. 4(a).

This data set was least-squares fitted using a Mie-Grüneisen model. In this model, the pressure is expressed as the sum of a "cold" (P_0) and thermal (P_{th}) part, i.e.,

$$P(V,T)=P_0(V)+P_{th}(V,T), \tag{4}$$

with $P_{th}(V,T)=0$ at 0 K. To represent $P_0(V)$, a Vinet equation[27] is used, whereas the thermal part is written in the Debye-Grüneisen (quasiharmonic) approximation using Eqs. (2) and (3). In this approximation, we have the identity $\gamma_{th}=\hat{\gamma}=\gamma_D$, where $\gamma_D=-\partial\ln(\Theta)/\partial\ln(V)$ is the Debye-Grüneisen parameter. The variation of the Debye temperature Θ with volume is thus given by that of γ_{th}. Here, γ_{th} was allowed to vary with the compression ratio according to the empirical relation $\gamma_{th}=\gamma_{th,0}(V/V_{0,0})^q$, where q was taken as constant.[42] In the fit, the only varying parameter is q. All the others ($V_{0,0}$, $B_{0,0}$, $B'_{0,0}$, $\gamma_{th,0}$, and Θ_0) were fixed to the values determined as described above. The obtained value for q is 4 ± 1.5, and the whole parameter set is given in Table V. Figure 4(b) shows the difference between the experimental pressures and the one predicted by the present model. This difference is for most data points smaller than ±1 GPa, and the rms deviation is 0.6 GPa. If we allow $B_{0,0}$ and $\gamma_{th,0}$ to vary in the fitting procedure, the resulting values are identical to the starting ones within their standard deviations. The parameter set given in Table V can thus be regarded as the best one for the Mie-Grüneisen EOS based on the present data.

The value found for q is large compared to the typical range for this parameter ($0.8<q<2.2$).[42] This is to be related to the rapid decrease of the thermal expansion coefficient with pressure that is observed from the present data. Indeed, γ_{th} and α are related by the thermodynamic relation $\alpha=(1/B)\gamma_{th}C_V$. In the quasiharmonic approximation, γ_{th} may be obtained by the Brillouin-zone integration of the phonon mode Grüneisen parameters. A large reduction of α may thus indicate that the Grüneisen parameters for the acoustic modes, which give the dominant contribution, rapidly decrease with pressure. As a matter of fact, the calculated γ for the transverse acoustic branches at $P=0$ are very low ($\sim$0.25) along some directions of the Brillouin zone, especially near the zone boundaries.[17] In diamond, which presents similar phonon dispersion curves, calculations show a decrease of these parameters with pressure, eventually leading to negative values of γ and α at ultrahigh pressures ($P>700$ GPa).[43] We also note that a similar phenomenon is responsible for the negative thermal expansion in Si at ambient pressure and low temperatures.[44] To illustrate the decrease of α with pressure, we plot in Fig. 5 its variation with temperature along several isobars from 0 to 100 GPa as deduced from the present Mie-Grüneisen EOS.

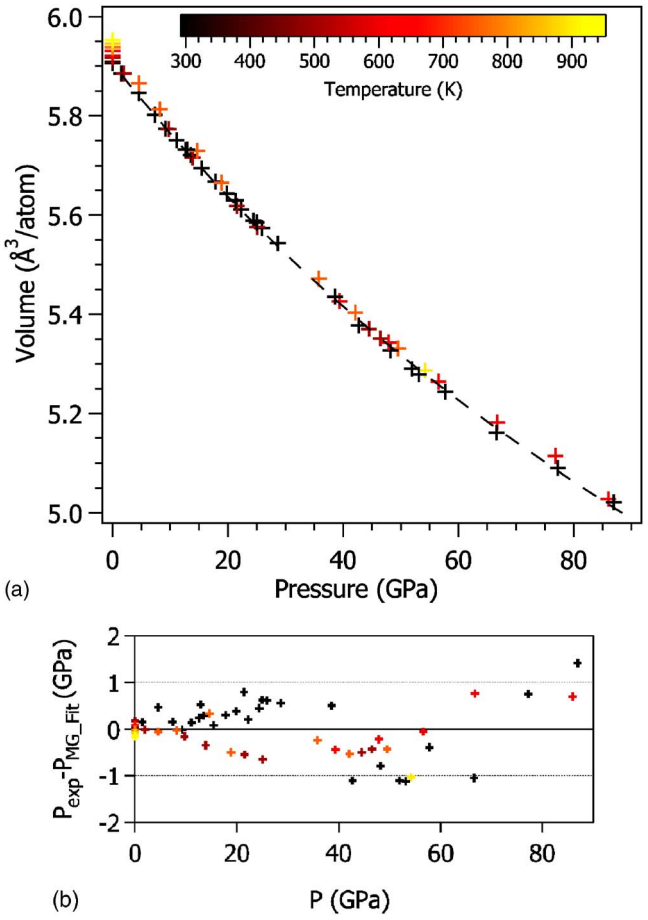

FIG. 4. (Color online) (a) Experimental volume of *c*-BN as a function of pressure and temperature obtained in the present work. Crosses show experimental data, and the dashed line is the Vinet fit to the data at 295 K. (b) Difference between experimental pressures and predicted ones using the Mie-Grüneisen model with the parameters given in Table V.

TABLE V. Parameters for the P-V-T equation of state of c-BN based on a Mie-Grüneisen model, with a Vinet equation (Ref. 27) for the static part and a Debye-Grüneisen model for the thermal part [Eq. (4)].

$V_{0,0}$, (Å^3/at.)	$B_{0,0}$ (GPa)	$B'_{0,0}$	Θ_0 (K)	$\gamma_{\mathrm{th},0}$	q
5.9026(4)	397(2)	3.62(5)	1700	1.04(2)	4(1.5)

VI. CONSTRAINED RAMAN PRESSURE SCALE

A. Temperature dependence of the TO mode Grüneisen parameter

The present construction of a P-V-T EOS enables us to reanalyze our previous measurements[3] of the Raman TO mode at HP-HT. In particular, we are now able to precisely determine the isothermal mode Grüneisen parameter $\gamma^{TO}(T)=-(\partial \ln \nu^{TO}/\partial \ln V)_T$, where ν^{TO} is the frequency of the TO mode. To do so, the sample volume was calculated for each P-T condition at which ν^{TO} was measured (see Ref. 3) by inverting Eq. (4).

The results are reported in Fig. 6, where we plot the experimental values of $\ln(\nu^{TO})$ as a function of $\ln[V/V_0(T)]$. In the scanned pressure range ($P<21$ GPa) and for each of the five studied isotherms ($300<T<723$ K), these two quantities appear to be linearly related. This tells us that $\gamma^{TO}(T)$ is constant along each isotherm and may then be directly determined by a linear regression of the data using the expression

$$\ln \nu^{TO}(V,T) = -\gamma^{TO}(T)\ln\frac{V(P,T)}{V_0(T)} + \ln \nu_0^{TO}(T), \qquad (5)$$

where $\nu_0^{TO}(T)=\nu^{TO}(P=0,T)$. The fits to the latter equation are shown as dotted lines in Fig. 6. The values of $\gamma^{TO}(T)$ and $\nu_0^{TO}(T)$ so obtained are listed in Table VI. It can be seen that, within error bars, $\gamma^{TO}(T)$ is constant in this P-T range, with an average value of 1.257(5). This value is slightly larger than that given by Aleksandrov *et al.*[1] (1.188) and in good agreement with the theoretical determination of Kern *et al.*[17] (1.2).

It can also be observed that $\nu_0^{TO}(T)$ follows $V_0(T)$ in a linear way in the probed T range. Extrapolating this line to 0 K gives a value of ν_0^{TO} at zero temperature of 1055.1(1) or 1054.6(2) cm^{-1}, depending on whether the fitted or experimental $\nu_0^{TO}(T)$ is used.

B. High-temperature pressure scale

In Ref. 3, we recalled the various reasons that make c-BN a good candidate for pressure measurement in a diamond-anvil cell at high temperature. A pressure scale was given based on the measurements of the TO mode frequency (ν^{TO}) at high P-T. The form of this pressure scale derives from the first-order Murnaghan EOS and is obtained by inverting the following equation for the P-T dependence of ν^{TO}:

$$\nu^{TO}(P,T) = \nu_0^{TO}(T)\left(1+\frac{B'_0}{B_0(T)}P\right)^{\gamma_{TO}/B'_0}. \qquad (6)$$

In Ref. 3, $B_0(T)$ and B'_0 were considered as fit parameters, taking for γ^{TO} the value reported by Ref. 1. We assumed then that γ^{TO} was independent of temperature, which is confirmed by the present work. Our EOS allows us to better constrain Eq. (6) by imposing physical constraints on the various pa-

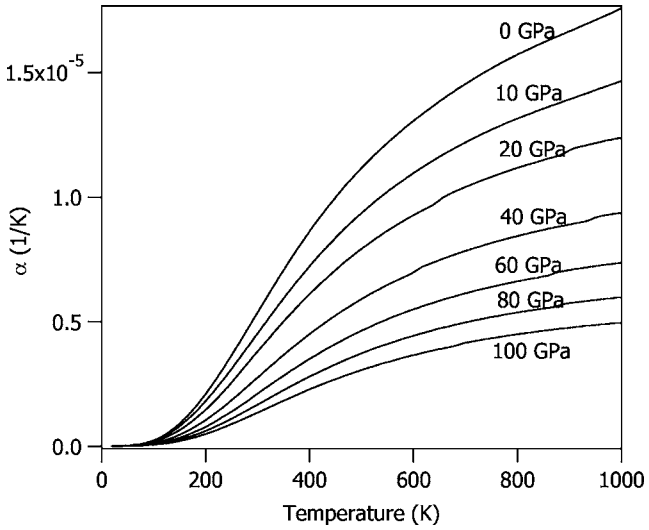

FIG. 5. Variation of the thermal expansion coefficient with temperature along several isobars, as deduced from the Mie-Grüneisen EOS.

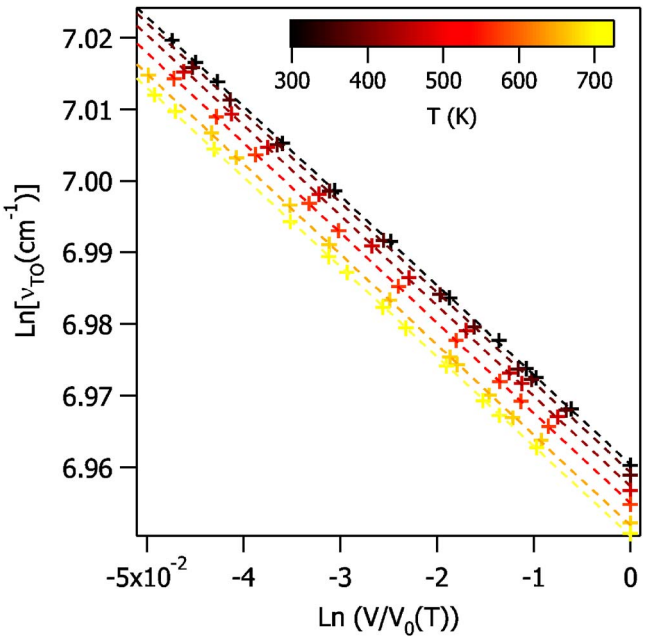

FIG. 6. (Color online) Frequencies of the TO Raman mode as a function of $V/V_0(T)$ on a logarithmic scale. The crosses show experimental data (Ref. 13) and the dashed lines are linear fits.

TABLE VI. Isothermal mode Grüneisen parameter of the Raman TO mode based on the Raman data reported in Ref. 3 and present P-V-T data. V_0 is the volume at $P=0$ obtained by inverting Eq. (4). The value of $\nu_0^{TO} \equiv \nu^{TO}(P=0,T)$ predicted by the linear regression of the data [Eq. (5)] is also given and compared to the direct measurements. T is in K, V_0 in Å^3/at., and ν_0^{TO} in cm^{-1}. The values at $T=0$ are obtained by linear regression of $\nu_0^{TO}(T)$ vs $V_0(T)$.

T	V_0	ν_0^{TO} (fit)	ν_0^{TO} (expt.)	γ^{TO} (fit)
300	5.9055	1054.0(1)	1053.93(10)	1.251(3)
373	5.9084	1052.9(2)	1052.43(20)	1.256(5)
473	5.9139	1050.8(2)	1050.17(13)	1.262(6)
573	5.9209	1048.3(1)	1048.17(27)	1.259(2)
673	5.9290	1045.1(1)	1045.45(13)	1.262(4)
723	5.9334	1043.6(1)	1043.91(41)	1.253(4)
0	5.9026	1055.1(1)	1054.6(2)	

rameters. Since this pressure scale is to be used for high temperatures, we only consider variations above 300 K. The variation of B_0 with temperature was deduced from our Mie-Grüneisen EOS by fitting isotherms at 100 K intervals by a Vinet equation. A quadratic form is found suitable to represent the behavior of B_0 between 300 and 2000 K, with the following expression:

$$B_0(T > 300\ \mathrm{K}) = 396.5(5) - 0.0288(14)(T-300) - 6.84(77)10^{-6}(T-300)^2. \quad (7)$$

The data for $\nu^{TO}(P,T)$ were then fitted to Eq. (6), using Eq. (7) as the expression for $B_0(T)$. Adding a temperature dependence to B_0' does not improve the fit, so we kept it as constant. The value of $\gamma^{TO}=1.257$ obtained above was used. As in Ref. 3, $\nu_0^{TO}(T)$ was expressed as a quadratic form, where the coefficients are allowed to vary within the boundaries given by Ref. 45. We thus obtain a revised pressure scale, reading as

$$P = \left(\frac{B_0(T)}{3.62}\right)\left\{\left[\frac{\nu^{TO}(P,T)}{\nu_0^{TO}(T)}\right]^{2.876} - 1\right\}, \quad (8)$$

with $B_0(T)$ as in Eq. (7) and $\nu_0^{TO}(T)=1058.4(5) - 0.0091(23)T - 1.54(22)\times 10^{-5}T^2$.

Recently, Goncharov *et al.*[5] reported Raman measurements up to 1750 K and 40 GPa in argon pressure medium and proposed a pressure scale in a form similar to Eq. (8). The two scales are compared in Fig. 7 in the pressure range 0–50 GPa at 300, 1000, and 1500 K. The difference increases with pressure and temperature and reaches ~10% at 50 GPa and 1000 K. The fact that the present scale is constrained by measured physical parameters gives us confidence that it can be safely used in the 0–100 GPa and 300–1000 K range. P-V-T as well as Raman data to higher T would be desirable to extend the calibration.

VII. CONCLUSIONS

We have reported experimental P-V-T data on c-BN from x-ray-diffraction experiments in a resistively heated diamond-anvil cell. Volume measurements extend to 160 GPa at 295 K and 80 GPa at 500–900 K. By fitting the room-temperature EOS to various EOS models, we extracted the values of the bulk modulus [395(2) GPa] and its first pressure derivative [3.62(5)]. We have also examined the variation of these parameters with respect to the chosen calibration of the ruby standard and showed that the one recently proposed by Holzapfel[11] (H2005) provides very good consistency between static compression data and *ab initio* predictions. Coupling the present information with independent measurements of B_0', such as obtained by sound-propagating experiments, would be of great interest to better constrain the ruby standard calibration in the megabar range. A good description of our full data set was obtained using a Mie-Grüneisen model, where the thermal pressure originating from lattice vibrational energy is calculated in the Debye approximation. We observe a rapid decrease of the thermal expansion coefficient with pressure, which itself reflects on the strong variation of the thermal Grüneisen parameter. The Mie-Grüneisen EOS was then used to determine the mode Grüneisen parameter of the Raman TO mode, which was found to be temperature independent in the range 300–723 K. A formulation of the Raman pressure scale was then deduced from the present results, which should hold in the P-T range 0–100 GPa and 300–1000 K. Extension of this work to higher temperatures would be valuable to better constrain the thermal effects and extend the calibration of the Raman scale.

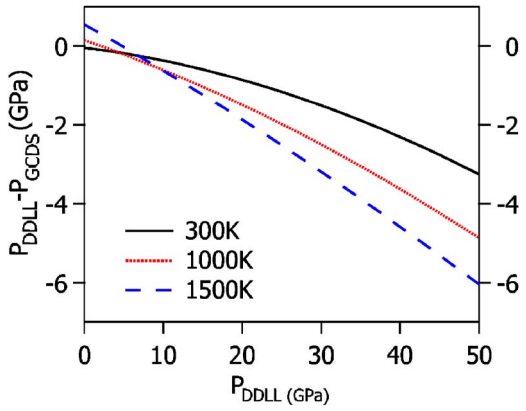

FIG. 7. (Color online) Comparison between the present pressure scale [P_{DDLL}, Eq. (8)] and the one given by Goncharov *et al.* [P_{GCDS}, Ref. 5, Eq. (2)]. The solid, dotted, and dashed lines show the difference between the two predicted pressures vs P_{DDLL} at, respectively, 300, 1000, and 1500 K.

ACKNOWLEDGMENTS

We thank V. L. Solozhenko for providing us with c-BN samples, B. Canny (IMPMC) for his help in preparing the experiments, and M. Mezouar (ESRF ID27) for his help during the x-ray-diffraction runs. The authors acknowledge the European Synchrotron Radiation Facility for provision of synchrotron radiation facility during beam time allocated to proposal HS-2514.

*Email address: datchi@impmc.jussieu.fr

[1] I. V. Aleksandrov, A. F. Goncharov, S. M. Stishov, and E. V. Yakovenko, JETP Lett. **50**, 127 (1989).
[2] M. Eremets, *High Pressure Experimental Methods* (Oxford University Press, Oxford, 1996).
[3] F. Datchi and B. Canny, Phys. Rev. B **69**, 144106 (2004).
[4] T. Kawamoto, K. Matsukage, T. Nagai, K. Nishimura, T. Mataki, S. Ochiai, and T. Taniguchi, Rev. Sci. Instrum. **75**, 2451 (2004).
[5] A. F. Goncharov, J. C. Crowhurst, J. K. Dewhurst, and S. Sharma, Phys. Rev. B **72**, 100104(R) (2005).
[6] W. Holzapfel, J. Appl. Phys. **93**, 1813 (2003).
[7] F. Occelli, P. Loubeyre, and R. LeToullec, Nat. Mater. **2**, 151 (2003).
[8] K. Kunc, I. Loa, and K. Syassen, Phys. Rev. B **68**, 094107 (2003).
[9] A. Dewaele, P. Loubeyre, and M. Mezouar, Phys. Rev. B **70**, 094112 (2004).
[10] A. D. Chijioke, W. J. Nellis, A. Soldatov, and I. F. Silvera, J. Appl. Phys. **98**, 114905 (2005).
[11] W. B. Holzapfel, High Press. Res. **25**, 87 (2005).
[12] P. I. Dorogokupets and A. R. Oganov, Phys. Rev. B **75**, 024115 (2007).
[13] V. L. Solozhenko, D. Haüsermann, M. Mezouar, and M. Kunz, Appl. Phys. Lett. **72**, 1691 (1998).
[14] E. Knittle, R. M. Wentzcovitch, R. Jeanloz, and M. L. Cohen, Nature (London) **337**, 349 (1989).
[15] K. Takemura, J. Appl. Phys. **89**, 662 (2001).
[16] K. Albe, Phys. Rev. B **55**, 6203 (1997).
[17] G. Kern, G. Kresse, and J. Hafner, Phys. Rev. B **59**, 8551 (1999).
[18] T. Tohei, A. Kuwabara, F. Oba, and I. Tanaka, Phys. Rev. B **73**, 064304 (2006).
[19] F. Datchi, P. Loubeyre, and R. LeToullec, Phys. Rev. B **61**, 6535 (2000).
[20] V. M. Giordano, F. Datchi, and A. Dewaele, J. Chem. Phys. **125**, 054504 (2006).
[21] H. K. Mao, J. Xu, and P. M. Bell, J. Geophys. Res. **91**, 4673 (1986).
[22] F. Datchi, R. LeToullec, and P. Loubeyre, J. Appl. Phys. **81**, 3333 (1997).
[23] P. Loubeyre, R. LeToullec, M. Hanfland, L. Ulivi, F. Datchi, and D. Hausermann, Phys. Rev. B **57**, 10403 (1998).
[24] A. Hammersley, S. Svensson, M. Hanfland, A. Fitch, and D. Hausermann, High Press. Res. **14**, 235 (1996).
[25] R. H. Wentorf, Jr., J. Chem. Phys. **26**, 956 (1957).
[26] T. Holland and S. Redfern, Miner. Mag. **61**, 65 (1997).
[27] P. Vinet, J. Ferrante, J. Rose, and J. Smith, J. Geophys. Res. **92**, 9319 (1987).
[28] F. Birch, J. Geophys. Res. **83**, 1257 (1978).
[29] W. Holzapfel, Z. Kristallogr. **216**, 473 (2001).
[30] G. A. Slack and S. F. Bertram, J. Appl. Phys. **46**, 89 (1975).
[31] M. Grimsditch, E. S. Zouboulis, and A. Polian, J. Appl. Phys. **76**, 832 (1994).
[32] H. J. McSkimin and P. Andreatch, J. Appl. Phys. **43**, 2944 (1972).
[33] R. Vogelgesang, A. K. Ramdas, S. Rodriguez, M. Grimsditch, and T. R. Anthony, Phys. Rev. B **54**, 3989 (1996).
[34] P. Pavone, K. Karch, O. Schütt, W. Windl, D. Strauch, P. Giannozzi, and S. Baroni, Phys. Rev. B **48**, 3156 (1993).
[35] K. Karch and F. Bechstedt, Phys. Rev. B **56**, 7404 (1997).
[36] R. Maezono, A. Ma, M. D. Towler, and R. J. Needs, Phys. Rev. Lett. **98**, 025701 (2007).
[37] J. Furthmüller, J. Hafner, and G. Kresse, Phys. Rev. B **50**, 15606 (1994).
[38] Y.-N. Xu and W. Y. Ching, Phys. Rev. B **44**, 7787 (1991).
[39] D. C. Wallace, *Thermodynamics of Crystals* (Wiley, New York, 1972).
[40] P. Gielisse, S. Mitra, J. Plendl, R. Griffis, L. Mansur, R. Marchall, and E. Pascoe, Phys. Rev. **155**, 1039 (1967).
[41] V. L. Solozhenko, V. Z. Turkevich, and W. B. Holzapfel, J. Phys. Chem. B **103**, 2903 (1999).
[42] O. L. Anderson, J. Geophys. Res. **84**, 3537 (1979).
[43] J. Xie, S. P. Chen, J. S. Tse, S. de Gironcoli, and S. Baroni, Phys. Rev. B **60**, 9444 (1999).
[44] C. H. Xu, C. Z. Wang, C. T. Chan, and K. M. Ho, Phys. Rev. B **43**, 5024 (1991).
[45] H. Herchen and M. A. Cappelli, Phys. Rev. B **47**, 14193 (1993).